

An Online Calibration System for Digital Input Electricity Meters Based on Improved Nuttall Window

Zhenhua Li^{1,2}, Yawei Du¹, A. Abu-Siada³, *Senior Member, IEEE*, Gang Bao¹, Jie Yu¹, and Tao Zhang¹

¹College of Electrical Engineering & New Energy, China Three Gorges University, Yichang 443002, China

²Hubei Provincial Engineering Technology Research Center for Microgrid, China Three Gorges University, Yichang 443002, China;

³Department of Electrical and Computer Engineering, Curtin University, Perth 6000, W.A., Australia

Corresponding author: Zhenhua Li (e-mail: lizhenhua1993@163.com).

This work was supported by China Scholarship Council, National Natural Science Foundation of China (Grant Number 51507091) and Key project of science and technology research plan of Education Department of Hubei (Grant Number D20181204).

ABSTRACT This paper proposes an improved online calibration technique for digital input electricity meters. The technique employs a double spectral line interpolation fast Fourier transform algorithm with four-item, three-order Nuttall window to reduce the measurement error caused by spectrum leakage, frequency fluctuation, noise pollution and harmonic interference. A calibration system of friendly human-computer interaction is designed using LabVIEW. Simulation and practical results show that the proposed calibration system with improved Nuttall window algorithm is of high accuracy and reliability when compared with the traditional calibration algorithm currently used by industry practice.

INDEX TERMS Digital input electricity meters, Online calibration system, Harmonic measurement, Four-item, three-orders Nuttall window

I. INTRODUCTION

Digital input electricity meter represents a key element in digital substations as its accuracy and reliability affirm the security of the power grid [1-3]. Owing to the fact that a digital substation is equipped with several power electronic devices and nonlinear loads, the harmonic contents within the voltage and current waveforms are substantial. Therefore, further improvement in the measurement accuracy of the digital input electricity meters has become essential. This can be done through adopting a cost-effective online calibration process for the digital meters. High accuracy calibration method can effectively suppress the influence of frequency fluctuation and harmonic interference on the measurements [4, 5].

In [6], a novel low-cost field instrument data calibration technique is proposed. This technique employs a relatively low-precision commercial energy meter as a calibrator along with SIMEX measurement error model and Bayesian regression to improve parameters estimation. Reference [7] mainly studies the key technologies, digital measurement systems and calibration methods of intelligent substation. The phase shift introduced by current transformers is a key

cause of measurement error, especially in the case of light loads. This issue is investigated in [8] in which an effective digital correction algorithm based on piecewise Lagrangian interpolation to reduce the phase shift of static instruments is introduced. However, the influences of harmonics, inter-harmonics and frequency fluctuation are not considered in this study. Reference [9] proposes a new structure of a smart meter with integrated calibration card to perform the calibration process remotely. However, the maintenance of standard sensors brings new problems. Furthermore, frequency fluctuations and harmonic interference are not considered. In reference [10] a theoretical quantitative analysis of the energy measurement error due to harmonic contents in the current and voltage waveforms is presented without practical validation.

Majority of existing measurement methods utilize conventional fast Fourier transform (FFT) algorithm to analyze voltage and current signals equipped with harmonic components. However, FFT algorithm is influenced by the frequency fluctuation that may result in reduced measurement accuracy [10]. As such, an FFT-based technique along with error correction algorithm has been presented in

[11-14] to improve the measurement accuracy for signals with substantial harmonic contents. In [11], based on a suitable lookup table, a fast interpolation method independent of window type and order is proposed. An FFT-based technique along with error correction algorithm has been presented in [12] to improve the measurement accuracy for signals with substantial harmonic contents. In [13], a new method for extracting and measuring a single harmonic of a time-varying frequency signal is proposed based on a nonlinear adaptive mechanism. In [14], an FFT-based harmonic measurement method for time-varying power systems is proposed.

In all of the above-proposed techniques, calibration accuracy level of 0.05 accuracy class was not guaranteed. To achieve calibration accuracy level of 0.05 accuracy class, the error correction algorithm should be improved further in a wide frequency band up to the 50th order harmonic components, which is the focus of this paper.

To realize high accuracy and online calibration of digital input electricity meters, this paper proposes a calibration technique based on four-item, three-order Nuttall window, which can realize effective online calibration for digital meters without switching them off. The proposed improved FFT algorithm is based on double spectral line interpolation with four-item, three-order Nuttall window. The proposed algorithm features faster side lobe attenuation speed and lower lobe peak level. The proposed technique has several advantages over the traditional FFT algorithm and it can realize effective inhibition of the spectrum leakage problem. Moreover, the proposed technique has good anti-interference ability and can reduce the errors caused by non-synchronous sampling and noise pollution, thus improving the measurement accuracy. The accuracy and stability of the proposed technique are verified through simulation analysis, experimental measurements and field-testing as will be elaborated below.

II. The Proposed Online Calibration System

As shown in Fig. 1, the proposed online calibration system contains a data acquisition card (DAQ), a power source, a network card and a multi-function software platform. The DAQ card is used to collect the output pulses of the calibrated digital meter. The power source is used to power the pulses output terminals of the digital input electricity meters and adjust the electrical level of the pulses.

In the proposed online calibration system shown in Fig. 1, the error of the calibrated digital meter is calculated through the comparison of the meter's output electric energy pulse and the output of the merging unit (MU) which is obtained from MU redundant interface through an optical fiber and is considered as the standard reference signal. The output of the MU is acquired by the network card and is sent to the software platform. A double spectral line interpolation FFT algorithm with four-item, three-order Nuttall window is employed in the software platform to realize the analysis and calculation of the fundamental and harmonic components

within the voltage and current waveforms. The ratio error and phase error of the calibrated digital meter are calculated and displayed by the developed software. The hardware and software platforms are elaborated below.

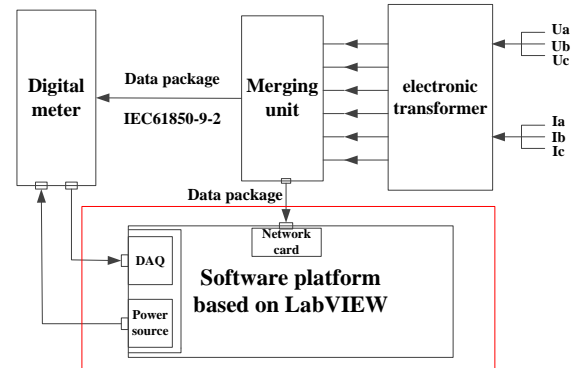


FIGURE 1 Structure of the proposed online calibration system for digital input electricity meters

A. Hardware platform

A Polar 9300M industrial personal computer (IPC) is utilized for the calibration software platform. IPC has good scalability, portability, anti-interference performance and is suitable for the field-testing.

To improve the resolution and sensitivity of the calibration system, a PCI-4474 DAQ card with 24-bits is used to realize the real time synchronous acquisition for multi-channel data. A DSA321SCA crystal oscillator is used as a synchronous clock to realize accurate synchronization of different channels.

Since the terminals of the digital meter are generally open-collector output terminals, power source and pull-up resistor are required to adjust its electrical level. The power supply circuit shown in Fig. 2 is equipped with a built-in 5 V DC source and pull-up resistors (R1 and R2) to supply the data acquisition channels.

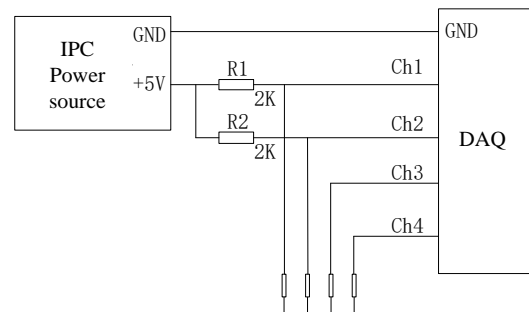


FIGURE 2 The self-powered circuit of PCI-4474

B. Software platform

The working logic diagram of the developed multi-function software platform is shown in Fig. 3 while the software interface is shown in Fig. 4. The main function of the software includes data collection, analysis and process, error calculation, wave display and data storage. The software provides measurement for the three-phase voltages, currents

and the error in the active and reactive power. There are four main parts in the software platform namely: parameter configuration, graph presentation, status display of the MU, and results calculation.

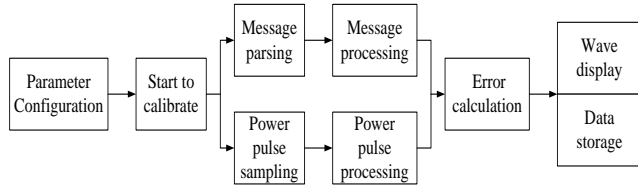


FIGURE 3 The working logic diagram of the software platform

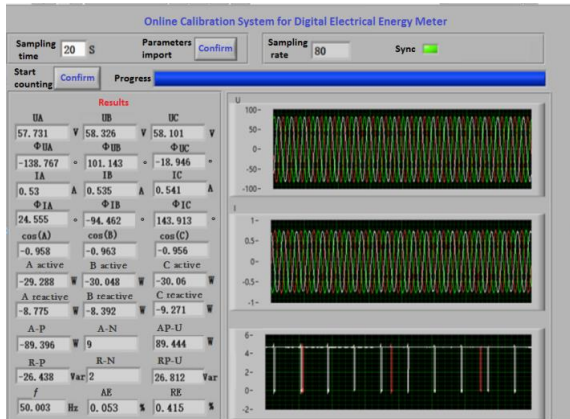


FIGURE 4 The software interface of the online calibration system

III. Electric Energy Measurement Algorithm

In this section, the mathematical equations of the proposed algorithm are briefly presented.

A. Four-item, three-order Nuttall window

Modern power grids are heavily equipped with power electronic devices and nonlinear loads that inject substantial levels of harmonics and inter-harmonics to the grids. When using conventional FFT algorithm to truncate the measurable signals such as current and voltage in the time domain under the case of non-synchronous sampling, significant error may arise due to the inherent spectral leakage and fence effect of the algorithm [15-18]. Hence, conventional FFT algorithm cannot meet the accuracy requirements of basic wave and harmonic energy measurement [19-22]. To solve this problem, several publications in the literatures propose the adoption of FFT algorithm with window interpolation, such as Blackman window [23-24], Hanning window [25-26] and triangular window [27-30]. Although these window functions can improve the calculation accuracy to some extent, their performance is not acceptable when a high measurement accuracy is required for the fundamental and harmonic components in the measured waveform.

To reduce the spectrum leakage and improve the accuracy of the proposed online calibration system for the digital meter, a four-item, three-order Nuttall window with superior side lobe performance is proposed in this paper to conduct weighted calculation. Table I shows that the side lobe peak value of the four-item, three-order Nuttall window is -83 dB,

and the side lobe attenuation rate is 30 dB/Oct. Table I shows that the side lobe peak value is lower and the attenuation rate is faster when compared with other traditional window functions. This algorithm can further reduce the influence of spectrum leakage and ensure high accuracy for the fundamental and harmonic components measurement.

As a combinatorial convolution window function, the time domain expression of the four-item, three-order Nuttall window is given as:

$$w_N(n) = \sum_{i=0}^3 (-1)^i a_i \cos\left(\frac{2\pi ni}{N}\right) \quad n=0,1,\dots,N-1 \quad (1)$$

The frequency domain expression using Fourier transform is:

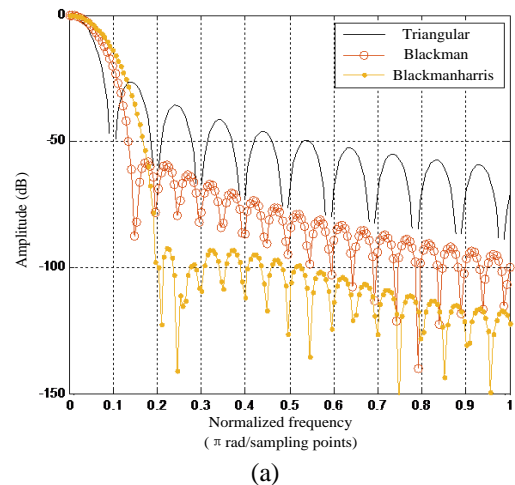
$$W(\omega) = \sum_{i=0}^3 (-1)^i \frac{a_i}{2} \left[W_R\left(\omega - \frac{2\pi i}{N}\right) + W_R\left(\omega + \frac{2\pi i}{N}\right) \right] \quad (2)$$

where, $a_0=0.338946$, $a_1=0.481973$, $a_2=0.161054$, $a_3=0.018027$, N is the number of samples, $W_R(\omega)$ is the spectral function of the rectangular window.

TABLE I
SIDE LOBE PERFORMANCE OF SEVERAL WINDOW FUNCTIONS

Window functions	main lobe width	Side lobe peak (dB)	Side lobe attenuation rate (dB/oct)
Triangular	$8\pi/N$	-27	12
Hamming	$8\pi/N$	-43	6
Blackman	$12\pi/N$	-59	18
Blackman-Harris	$16\pi/N$	-92	6
Hanning	$8\pi/N$	-32	18
Four item three order Nuttall	$16\pi/N$	-83	30

The magnitude-frequency characteristic of the commonly used window functions and the four-item, three-order Nuttall window is shown in Fig. 5. As can be seen in the figure, for the same number of sampling points, the side lobe attenuation rate of the improved Nuttall window is about 2-5 times that of other window functions, as a result, the effects of spectrum leakage can be effectively suppressed.



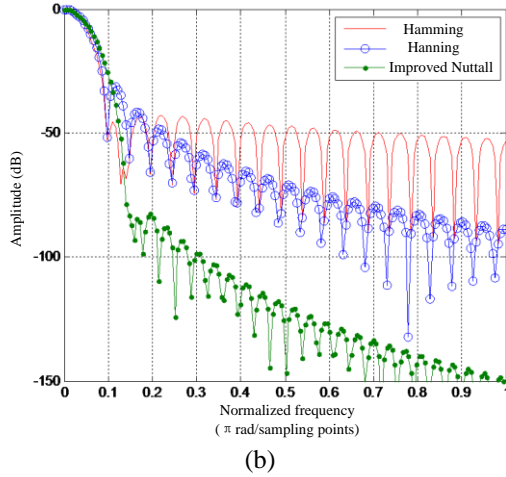


FIGURE 5 The amplitude-frequency characteristics of different window functions (a) Commonly used window functions (b) Improved Nuttall window and rising-cosine functions

B. Double spectral line interpolation FFT algorithm with four-item, three-order Nuttall window

The conventional FFT algorithm deviates the calculated frequency of the measured signals from the original frequency and measurement error arises due to the fence effect caused by non-synchronous sampling [31, 32]. As a result, a double spectral line interpolation FFT algorithm is proposed below to modify the amplitude and phase angle and hence improving the measurement accuracy.

In the discrete spectrum after the k_{th} harmonic signal is added with the window function, let the maximum and the second largest spectral line of the samples obtained near the accurate frequency point of the k_{th} harmonic order be k_m and k_{m+1} , and the corresponding amplitudes to be y_m and y_{m+1} , respectively. Let $\beta = (y_{m+1} - y_m) / (y_{m+1} + y_m)$.

The frequency deviation ε can be obtained using polynomial fitting:

$$\varepsilon = f_\varepsilon(\beta) = 0.0923069\beta^5 + 0.1767194\beta^3 + 2.95494514\beta + 0.5 \quad (3)$$

Thereby, the phase angle (φ_0) and the amplitude (A_0) correction formulas of the harmonic signal can be obtained from:

$$\varphi_0 = \arg[X(k_i\Delta f)] - \pi[\varepsilon - 0.5(1 + (-12)^{i-m+1}) + \frac{\pi}{2}] \quad (i = m, m + 1) \quad (4)$$

$$A_0 = \frac{y_m + y_{m+1}}{N} (0.14734229\varepsilon^4 - 0.29468448\varepsilon^3 + 1.139752735\varepsilon^2 - 0.992410445\varepsilon + 3.44865515) \quad (5)$$

where, $\Delta f = f_s/N$, is the ratio of the sampling frequency to the sampling number.

It is to be noted that a double spectral line interpolation FFT algorithm is proposed because of its advantageous over

the three spectral line interpretation method that exhibits large calculation time and complexity. Moreover, the three spectral line interpretation method does not consider the information near the frequency symmetry line, which reduces its accuracy [REF].

IV. Simulation Analysis

In this section, the accuracy of the proposed algorithm is verified through extensive simulation analysis.

A. Error of harmonic energy measurement

In order to verify the reliability and accuracy of the harmonic energy measurement algorithm used in the calibration system, error simulation analysis is carried out. The signal of the MU exhibits a substantial level of harmonic components due to the electromagnetic interference within the substation. Therefore, for better simulation of the substation site, the voltage and current signals are set as:

$$u(n) = \sum_{k=1}^9 U_k \sin(2\pi k f_0 n / f_s + \varphi_{uk}) \quad (6)$$

$$i(n) = \sum_{k=1}^9 I_k \sin(2\pi k f_0 n / f_s + \varphi_{ik}) \quad (7)$$

where, the fundamental frequency $f_0 = 50\text{Hz}$, the sampling frequency $f_s = 6400\text{Hz}$, the number of samples $n = 1024$.

The detailed parameters of the voltage and current signals are listed in Table II.

TABLE II
PARAMETERS OF SIMULATED VOLTAGE AND CURRENT SIGNALS

k	$U_k(\text{V})$	$\varphi_{uk}(\text{°})$	$I_k(\text{A})$	$\varphi_{ik}(\text{°})$
1	200.5	10	10	31
2	4.4	35	0.15	5
3	3.5	68	0.8	64
4	0.9	46	0.12	77
5	2.1	20	0.65	51
6	0.5	85	0.1	15
7	1.3	51	0.48	62
8	0.4	28	0.05	37
9	1.1	52	0.32	53

To verify the accuracy of the proposed algorithm, simulation analysis is conducted by adding different window functions, such as Blackman-Harris window, four-order triangular self-convolution window, and four-item three-order Nuttall window. The relative error of the active power measurement using each method is calculated as shown in Table III based on the following equation:

$$\varepsilon_p = \frac{P_c - P_s}{P} \times 100\% \quad (8) \text{ please re-write}$$

where, ε_p is the error of the calibration system, P_c is the output power value of the calibration system, and P_s is the output power value of the standard energy metering device.

In each window function, calculation is conducted with and without the use of double line interpolation correction. As can be seen from Table III, the measurement accuracy can

be substantially improved by using interpolation. Compared with Blackman-Harris window and four-order triangular self-convolution window, the interpolation FFT algorithm based on improved Nuttall window has higher measurement accuracy for harmonic active power measurement. In particular, for the 2nd, 6th, 8th harmonic components that are relatively close to the fundamental component, the proposed algorithm has less error, compared with the four-order triangular self-convolution window. As a result, the proposed technique can effectively inhibit the calculation error caused by mutual interference between adjacent harmonic signals.

TABLE III
MEASUREMENT ERROR OF ACTIVE POWER

	Blackman-Harris		Four order triangular self-convolution		Four item three order Nuttall	
	without correction	with correction	without correction	with correction	without correction	with correction
$P_1(\%)$	3.78E-2	6.31E-5	2.11E-3	-1.58E-6	-7.95E-2	-6.39E-4
$P_2(\%)$	56.01	12.0	8.37	-4.7E-1	1.21E-1	-1.27E-2
$P_3(\%)$	17.35	3.08	-6.61E-1	-4.04E-3	3.21E-2	1.12E-4
$P_4(\%)$	13.62	-2.04	-1.82E-2	-3.18E-3	-2.56E-2	-7.66E-3
$P_5(\%)$	-78.4	-50.1	3.87E-1	9.03E-3	3.01E-2	-3.0E-4
$P_6(\%)$	56.21	30.9	-3.66	-2.7E-2	4.45E-1	-1.84E-2
$P_7(\%)$	-67.8	-31.4	5.65E-1	2.01E-2	3.67E-2	5.13E-4

$P_8(\%)$	32.55	6.09	3.21E-1	6.1E-3	-1.02E-3	-3.36E-5
$P_9(\%)$	3.21E-1	1.14E-3	-7.71E-2	-1.01E-5	-8.92E-2	-1.95E-4

B. Simulation under different interferences

It is inevitable that the measurement accuracy of electric energy is affected by the frequency fluctuation, noise pollution and harmonic change in an actual environment. To verify the anti-interference performance of the proposed calibration algorithm, the following simulations are carried out.

(1) *Frequency fluctuation*: In this case study, the power frequency is varied within the range $\pm 10\%$ (i.e. 49.5 to 50.5 Hz). It can be seen from the results listed in Table IV that the measurement error of the harmonic active power is affected by the fluctuation of the power frequency and the largest error is less than 0.02%.

(2) *Noise pollution*: In this case, the signal is superimposed with a white noise in the range of 20 to 60 dB and the results are listed in Table V. Results show that white noise influences the energy measurement accuracy.

(3) *Spectrum leakage and fence effect*: This case is simulated by maintaining the phase angle of the original voltage and current signals and varying the amplitudes of each harmonic component. Results in Table VI reveal that when the harmonic components are changed, the accuracy of the electric energy measurement is almost unaffected.

TABLE IV
POWER ERROR MEASUREMENT UNDER POWER FREQUENCY FLUCTUATION

	$P_1(\%)$	$P_2(\%)$	$P_3(\%)$	$P_4(\%)$	$P_5(\%)$	$P_6(\%)$	$P_7(\%)$	$P_8(\%)$	$P_9(\%)$
49.5Hz	3.83E-4	5.26E-2	-7.11E-2	-9.49E-2	-4.76E-2	-2.68E-2	-1.29E-4	-5.48E-3	-9.04E-4
49.7Hz	-2.46E-4	5.62E-2	-1.21E-2	1.3E-2	-3.5E-2	-9.59E-2	-8.67E-2	-1.18E-2	-1.83E-2
49.9Hz	-6.43E-4	6.86E-2	-4.64E-3	7.31E-4	-8.41E-3	-2.33E-2	-1.53E-2	-1.7E-2	-2.31E-2
50Hz	-1.2E-3	-1.3E-2	-1.25E-3	-1.5E-3	-1.23E-3	-1.6E-2	-1.24E-3	-7.5E-4	-1.26E-3
50.3Hz	-1.19E-4	-4.56E-2	4.17E-5	-2.17E-2	-2.44E-3	-1.23E-2	-5.3E-4	-7.03E-3	-1.26E-4
50.5Hz	3.68E-4	-8.74E-2	-1.03E-3	-5.14E-4	-2.88E-2	-3.37E-2	-2.56E-2	-3.9E-2	-1.06E-2

TABLE V
POWER ERROR MEASUREMENT UNDER SIGNAL WHITE NOISE

	$P_1(\%)$	$P_2(\%)$	$P_3(\%)$	$P_4(\%)$	$P_5(\%)$	$P_6(\%)$	$P_7(\%)$	$P_8(\%)$	$P_9(\%)$
20dB	-1.24E-2	9.02E-2	6.26E-2	4.02E-2	-1.28E-2	4.59E-2	-6.25E-2	-4.11E-2	-7.92E-2
30dB	8.85E-3	4.82E-2	5.54E-3	-2.51E-2	1.17E-3	3.02E-2	-2.03E-3	1.18E-2	-7.91E-3
40dB	4.17E-3	1.05E-2	-9.38E-3	1.37E-3	-6.99E-3	3.07E-2	-5.01E-3	-9.01E-3	3.19E-4
50dB	-1.07E-3	-4.14E-2	-3.72E-3	2.25E-2	5.23E-3	-2.89E-2	1.29E-3	-7.45E-3	2.41E-4
60dB	5.48E-4	-9.07E-2	1.97E-3	1.97E-2	1.85E-3	-2.43E-2	1.96E-4	-3.47E-3	4.11E-3

TABLE VI
POWER ERROR MEASUREMENT UNDER HARMONIC CHANGES

	$P_1(\%)$	$P_2(\%)$	$P_3(\%)$	$P_4(\%)$	$P_5(\%)$	$P_6(\%)$	$P_7(\%)$	$P_8(\%)$	$P_9(\%)$
-50%	-6.43E-4	-3.26E-2	-1.84E-5	-4.71E-4	4.13E-4	1.07E-4	1.51E-4	-4.42E-6	1.82E-4
-20%	-6.44E-4	-2.27E-2	-1.15E-5	-1.56E-4	3.23E-4	6.78E-5	4.51E-4	1.30E-5	1.14E-4
Original signal	-6.38E-4	-1.82E-2	1.93E-5	1.28E-4	3.01E-4	5.61E-5	3.61E-4	2.48E-4	9.09E-5

+20%	-6.36E-4	-1.10E-2	1.62E-5	-1.05E-4	2.91E-4	4.68E-5	3.65E-4	2.06E-4	9.09E-5
+50%	-6.13E-4	-1.22E-2	1.21E-4	-9.16E-6	3.67E-4	3.74E-5	3.43E-4	1.38E-4	1.21E-4

Fig. 6 shows the relative error in the 2nd harmonic component which is the most susceptible component to the interference with the fundamental component of the power signal under frequency fluctuation, white noise and variation of the harmonic components. Under the same conditions, traditional interpolation FFT algorithm based on Hanning and Blackman-Harris windows are vulnerable to external interference and the range of relative measurement error is large as can be seen in Fig. 6. For example, in Fig. 6 (b), the error for four-order triangular self-convolution window is 0.677% when the white noise is 40 dB while it is only 0.0105% for the four-item, three-order Nuttall window. This figure clearly shows that compared with other commonly used window functions, the interpolation FFT algorithm based on four-item, three-order Nuttall window has the lowest measurement error.

From the above results, it can be concluded that the proposed calibration system based on double spectral line interpolation FFT algorithm with four-item, three-order Nuttall window has better anti-interference performance. The proposed algorithm can effectively overcome the influence of frequency fluctuation, noise pollution and changes in harmonic components.

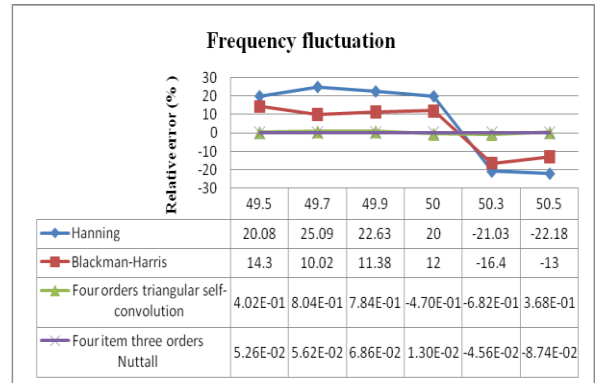
V. Experimental Measurements

In this section, the robustness of the proposed algorithm is verified through experimental measurements according to the relevant standards [33, 34].

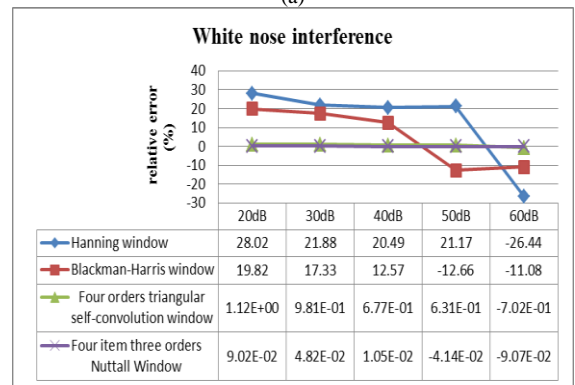
A. Accuracy test

To facilitate the accuracy calculation of the proposed online calibration system for the digital input electricity meters, its reading is compared with a standard power-metering device of 0.01 accuracy class as per the schematic of Fig. 7. According to the JJG597-2005 standards [33], accuracy tests should be conducted under different power factors, including unity, 0.5 lagging, 0.5 leading or 0.8 leading at different operating conditions. In addition, a power factor of 0.25 lagging may be conducted under very special requirements.

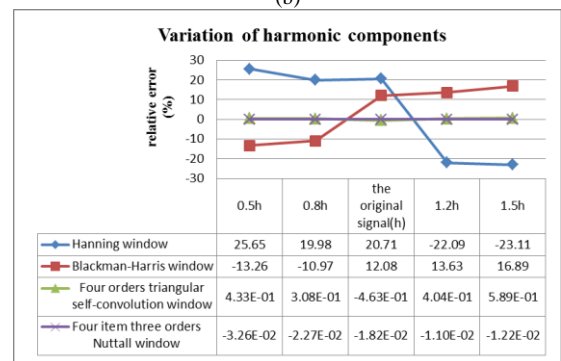
The results of the accuracy test are shown in Table VII under various source current and power factor levels. It can be seen that the error of the proposed system is less than 0.05% regardless the source current level and the power factor. On the other hand, results of the frequency fluctuation test is shown in Table VIII, considering the frequency fluctuation limits given in GB/T 15945-2008 standards [35]. From these results, one can see that the error of the calibration system is always less than 0.01% for power frequency variation in the range of 49 to 51 Hz.



(a)



(b)



(c)

FIGURE 6 The relative measurement error of the 2nd harmonic of the active power signal with different windows under (a) Frequency fluctuation (b) White noise (c) Variation of harmonic components

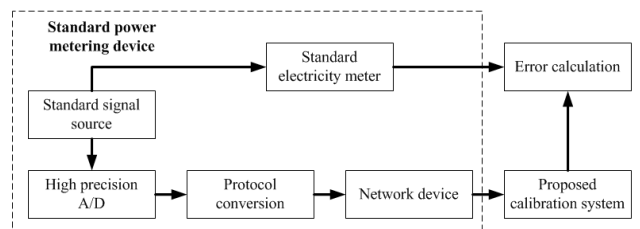


FIGURE 7 Accuracy test of the online calibration system

TABLE VII
ACCURACY TEST OF THE PROPOSED ONLINE CALIBRATION SYSTEM

Voltage (V)	Current (A)	Power factor	Error (%)	
110kV	1kA	1.0	-0.003	
		0.5 lagging	-0.003	
		0.5 leading	-0.003	
		1.0	-0.002	
		500A	0.5 lagging	-0.002
		0.5 leading	-0.002	
	100A	1.0	-0.001	
		0.5 lagging	-0.001	
		0.5 leading	-0.001	
		1.0	-0.002	
		50A	0.5 lagging	-0.002
		0.5 leading	-0.002	
10A	1.0	-0.001		
	0.5 lagging	-0.001		
	0.5 leading	-0.001		
	0.5 leading	-0.001		

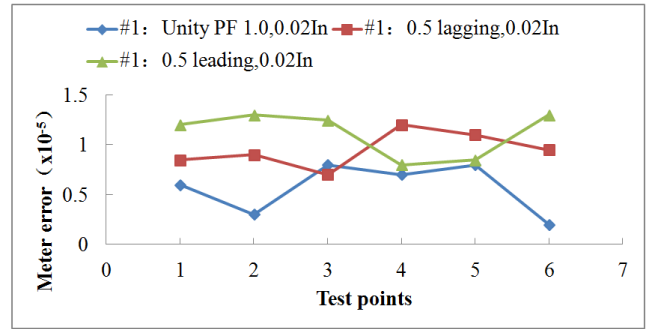
TABLE VIII
ERROR TEST OF FREQUENCY FLUCTUATION

Voltage (V)	Current (A)	Power factor	Frequency (Hz)	Error (%)
110kV	1kA	1.0	49Hz	0.002
			49.5Hz	0.002
			50Hz	0.001
			50.5Hz	0.000
			51Hz	-0.001
			51Hz	-0.001

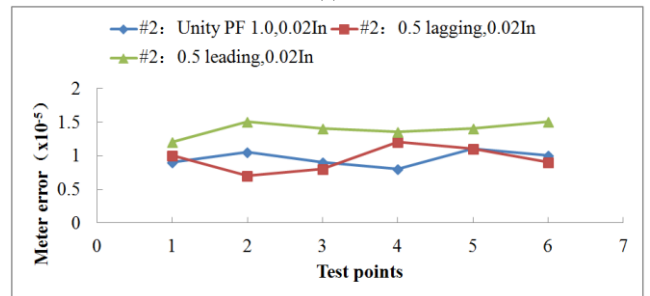
B. Engineering application

The proposed online calibration system has been successfully applied in several substations in Yichang Power Supply Company in China such as Songshan 110 kV substation and Donghu 110 kV substation in Yichang, Hubei province.

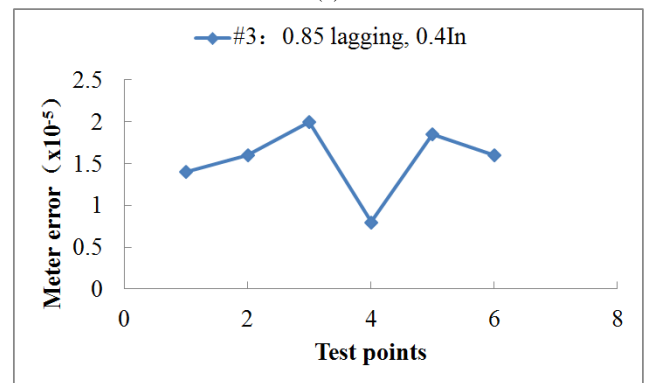
Fig. 8 shows the error variation of two digital electricity meters during the calibration process using the proposed algorithm in this paper. Fig. 8 (a) and (b) are offline tests that are conducted under a current level of $0.02I_n$ (I_n is the rated value, usually 5 A) and various source power factors (unity, 0.5 lagging and 0.5 leading). Fig. 8 (c) is the online calibration under a load of 0.85 lagging power factor at $0.4I_n$. All meters are of 0.2 accuracy class. From Figs. 8 (a) and (b) one can see that the error changes are less than 1.5×10^{-5} under power factor of 1.0, 0.5 lagging, and 0.5 leading. On the other hand, Fig. 8 (c) shows that the error changes are less than 2×10^{-5} . The test results show that the errors of the three investigated digital power meters are less than 0.01%, which meets the requirement of the 0.05 accuracy class.



(a)



(b)



(c)

FIGURE 8 Field test results of three operating digital meters (a) #1 Meter error (b) #2 Meter error (c) #3 Meter error

VI. Conclusion

This paper proposes an online calibration system based on double spectral line interpolation FFT algorithm with four-item, three-order Nuttall window. Results reveal the high accuracy and anti-interference capability of the proposed system, which can effectively realize the field calibration of digital electric energy meter. The key features of the proposed system can be summarized as below:

1) The utilization of a double spectral line interpolation FFT algorithm with improved Nuttall window which has a good side lobe performance can effectively suppress the spectrum leakage and fence effect of the conventional FFT algorithm and overcome the influence of frequency fluctuation, harmonic components variation and noise interference. As a result, the calibration accuracy can be improved.

2) The digital meter can be calibrated online without the need to switch it off as per the current practice. Hence the

calibration process is greatly simplified.

3) The software platform is designed using LabVIEW, which has strong versatility and friendly human-machine interaction performance.

4) The field test results show that the proposed calibration system is easy to operate and can meet the requirements of 0.05 accuracy class.

REFERENCES

- [1] M. Barbiroli, F. Fuschini, G. Tartarini, et al. "Smart Metering Wireless Networks at 169 MHz," *IEEE Access*, vol.5, no.99, pp.8357-8368, May.2017.
- [2] M. Urekar, D. Pejic, V. Vujicic, et al. "Accuracy improvement of the stochastic digital electrical energy meter," *Measurement*, vol.98, pp.139-150, Feb.2017.
- [3] S. M. S. Hussain, A. Tak, A. Ikbal, et al. "Communication Modeling of Solar Home System and Smart Meter in Smart Grids," *IEEE Access*, vol.6, pp.16985-16996, Feb.2018.
- [4] J. Wu and W. Zhao, "A simple interpolation algorithm for measuring multi frequency signal based on FFT," *Measurement*, vol.42, no.2, pp.322-327, Feb.2009.
- [5] G.W. Chang, C. I. Chen, and M.C. Wu, "Measuring power system harmonics and interharmonics by an improved fast Fourier transform based algorithm," *IET Generation Transmission Distribution*, vol.2, no.2, pp.193-201, Mar. 2008.
- [6] H. Carstens, X.H. Xia, and S. Yadavalli, "Low-cost energy meter calibration method for measurement and verification," *Applied Energy*, vol.188, pp.563-575, Feb.2017.
- [7] F. Zhou, Y.Y. Cheng, J. Xiao, et al. "Advanced Research & Technology in Industry Applic.," Ottawa, Ontario, Canada, Sep.2014.
- [8] J.M. Li, Z.S. Teng, Y. Wang, et al, "A Digital Calibration Approach for Reducing Phase Shift of Electronic Power Meter Measurement," *IEEE Transactions on Instrumentation and Measurement*, vol.67, no.7, pp.1638-1645, JUL.2018.
- [9] Z. Jebroni, H. Chadli, E. Chadli, et al, "Remote calibration system of a smart electrical energy meter," *Journal of Electrical Systems*, vol.13, no.4, pp.806-823, 2017.
- [10] Y.J. ZHANG and H. SHI, "Harmonic error modifying of electric energy meter considering harmonic responsivity," *Power System Protection and Control*, vol.37, no.22, pp. 58-61, Nov.2009.
- [11] A. Ferrero, S. Salicone, and S. Toscani, "A Fast, simplified frequency domain interpolation method for the evaluation of the frequency and amplitude of spectral components," *Measurement*, vol.60, no.5, pp.1579-1587, May.2011.
- [12] H. Wen, J.H. Zhang, and W.X. Yao, "FFT-Based Amplitude Estimation of Power Distribution Systems Signal Distorted by Harmonics and Noise," *IEEE Transactions on Industrial Informatics*, vol.14, no.4, pp. 1447-1455, Jan.2018.
- [13] M. Karimi-Ghartemani and M.R. Iravani, "Measurement of harmonics/inter-harmonics of time-varying frequencies," *IEEE Transactions Power Delivery*, vol.20, no.1, pp. 23-31, Jan.2005.
- [14] W.X. Yao, Z.S. Teng, and Q. Tang, "Measurement of power system harmonic based on adaptive Kaiser self-convolution window," *IET Generation Transmission & Distribution*, vol.10, no.2, pp.390-398, Sept.2015.
- [15] D. Amicone, A. Bernieri, and M. Laracca, "A smart add-on device for the remote calibration of electrical energy meters," *International Instrumentation and Measurement*, vol.42, no.3, pp.1599-1604, May. 2009.
- [16] F.S. Zhao, Z.X. Guo, and W. Yu, "The algorithm of interpolating windowed FFT for harmonic analysis of electric power system," *IEEE Transactions on Power Delivery*, vol.16, no.2, pp.160-164, Apr.2001.
- [17] L.M. Wang, Z.G. Zeng, M.F. Ge, et al, "Global stabilization analysis of inertial memristive recurrent neural networks with discrete and distributed delays," *Neural Networks*, vol.105, pp.65-74, Sep.2018.
- [18] K. Asif, M. Saim, and T. Pervez, "Analyzing Integrated Renewable Energy and Smart-Grid Systems to Improve Voltage Quality and Harmonic Distortion Losses at Electric-Vehicle Charging Stations," *IEEE Access*, vol.6, pp.26404-26415, Apr.2018.
- [19] W. He, S.T. Zhao, Y. Wang, et al. "Simple interpolated FFT algorithm based on minimize sidelobe windows for power harmonic analysis," *IEEE Transactions on Power Electronics*, vol.26, no.9, pp.2570-2579, Sept.2011.
- [20] L.M. Wang, Z.G. Zeng, J.H. Hu, et al, "Controller design for global fixed-time synchronization of delayed neural networks with discontinuous activations," *Neural Networks*, vol. 87, pp.122-131, Mar.2017.
- [21] A. Testa, D. Gallo, and R. Langella, "On the processing of harmonics and interharmonics: Using Hanning window in standard framework," *IEEE Transactions on Power Delivery*, vol.19, no.1, pp.28-34, Jan.2004.
- [22] T.X. Su, M.F. Yang, and J. Tao, "Power harmonic and interharmonic detection method in renewable power based on Nuttall double-window all-phase FFT algorithm," *IET Renewable Power Generation*, vol.12, no.8, pp.953-961, Jun.2018.
- [23] W.B. Tian and J.M. Yu, "Power system harmonic detection based on bartlett-hanning windowed FFT interpolation," *IEEE Transactions on Power Systems*, vol.12, no.2, pp. 4577-4579, May.2012.
- [24] R. Hyun-Joon, K. Nam-Kyun, R. Sangwon, et al. "Determination of electron energy probability function in low-temperature plasmas from current - Voltage characteristics of two Langmuir probes filtered by Savitzky-Golay and Blackman window methods," *Current Applied Physics*, vol.15, no.10, pp.1173-1183, Oct.2015.
- [25] H. Xue and R. Yang, "Optimal interpolating windowed discrete Fourier transform algorithms for harmonic analysis in power systems," *IEEE Transactions on Power Systems*, vol.40, no.7, pp.583-587, Aug.2003.
- [26] H. Wen, Z.S. Teng, S.Y. Guo, et al. "Hanning self-convolution window and its application to harmonic analysis," *Science China Series E-Technological*, vol.52, no.2, pp.467-476, Feb.2009.
- [27] H. Wen, Z.S. Teng, S.Y. Guo, et al. "Triangular self-convolution window with desirable side lobe behaviors for harmonic analysis of power system," *IEEE Transactions on Instrumentation Measurement*, vol.59, no. 3, pp.543-552, Jan.2004.
- [28] W. He, J.H. Zhang, and Z. Meng, "Harmonic Estimation Using Symmetrical Interpolation FFT Based on Triangular Self-Convolution Window," *IEEE Transactions on Industrial Informatics*, vol.11, no.1, pp.16-26, Feb.2015.
- [29] M. Meco-Gutierrez, J.R. Heredia-Larrubia, and F. Perez-Hidalgo, "Pulse width modulation technique parameter selection with harmonic injection and frequency-modulated triangular carrier," *IET Power Electronics*, vol.6, no.9, pp.54-62, 2013.
- [30] S. Zhu, Q.Q. Yang, Y. Shen, "Noise further expresses exponential decay for globally exponentially stable time-varying delayed neural networks," *Neural Networks*, vol.77, pp.7-13, May.2016.
- [31] D. Liu, S. Zhu, E. Ye, "Synchronization stability of memristor-based complex-valued neural networks with time delays," *Neural Networks*, vol.96, pp.115-127, Dec.2017.
- [32] M. Zdenek, and A. Martti, "HV impulse measuring systems analysis and qualification by estimation of measurement errors via FFT, convolution, and IFFT," *IEEE Transactions on Instrumentation and Measurement*, vol.54, no.5, pp.2013-2019, Oct.2005.
- [33] JJG597-2005 Verification Equipment for AC Electrical Energy Meters [S].

- [34] GB/T 17215.303-2013 Electricity metering equipment (a.c.)-Particular requirements-Part 3: Digital input electricity meters [S].
- [35] GB/T 15945-2008, Power quality-Frequency deviation for power system [S].